

CHLORINE ATOMIC CHAINS ON Ag(111) SURFACE

N.V. PETROVA, I.N. YAKOVKIN, O.M. BRAUN

PACS 68.43.Bc; 68.43.Fg
©2012Institute of Physics, Nat. Acad. of Sci. of Ukraine
(46, Prosp. Nauky, Kyiv 03028, Ukraine; e-mail: yakov@iop.kiev.ua)

The formation of chlorine chain structures on an Ag(111) surface is studied within the Monte-Carlo simulation method. Parameters of the lateral interaction calculated in the framework of density functional theory are used. The chain formation was shown to stem from the indirect interaction between chlorine adatoms owing to Friedel oscillations of the conduction electron concentration emerging when partially charged adatoms are screened. The numerical simulation allowed the formation of the experimentally observed sequence of chlorine structures on the Ag(111) surface to be explained. In particular, the mechanism of transformation from the chain structure into the hexagonal $(\sqrt{3} \times \sqrt{3})R30^\circ$ one as the coverage increases to $\theta = 0.33$ has been elucidated.

1. Introduction

Practical importance of a detailed study of the properties of chlorine layers adsorbed on a silver surface is associated, first of all, with the Cl ability to enhance the catalytic selectivity of the ethylene oxidation reaction, which is used in the chemical industry. Adsorption of Cl atoms onto the Ag (111) surface was widely studied by different experimental techniques, in particular, low-energy electron diffraction (LEED) [1–5], surface extended X-ray-absorption fine-structure spectroscopy (SEXAFS) [5, 6], thermal desorption [2, 3], Auger spectroscopy [1–3], scanning tunnel microscopy (STM) [4, 7–9], as well as theoretically in the framework of the electron density functional theory (DFT) and the Monte-Carlo simulation technique [10–16]. Adsorption of chlorine on the Ag(111) surface is associated with the dissociation of a Cl_2 molecule (it is an exothermic reaction characterized by an almost zero activation barrier [2]). The initial sticking coefficient of Cl atoms on the Ag(111) surface is 0.4 [4]. If the coverage does not exceed half a monolayer, chlorine atoms do not diffuse into the substrate at room temperature, thus remaining on the surface in the chemisorbed state [14, 17].

Recent researches of structures formed by chlorine atoms on the Ag(111) surface, which were carried out at a surface temperature of 5 K using the STM method [9], demonstrated that, in the coverage interval from 0.03 to 0.31, adatoms form chains, the length and the number of

which increase with the coverage degree. In particular, if this parameter is low, chlorine atoms create chain fragments characterized by identical interatomic distances of 4.4–4.5 Å (Fig. 1, *a*). At coverages θ higher than 0.25, the chain structures are formed simultaneously with islands of the $(\sqrt{3} \times \sqrt{3})R30^\circ$ structure (Fig. 1, *b*), and, at $\theta = 0.33$, almost the whole surface becomes occupied (this structure was observed within the LEED and STM methods [4, 5, 8]).

It is important to notice that the interatomic distances in the $(\sqrt{3} \times \sqrt{3})R30^\circ$ structure equal 5.01 Å, i.e. they considerably exceed the distance between chlorine adatoms in the chains that are created at lower coverage degrees. This feature testifies to a complicated character of the lateral interaction. Really, if one supposes that the attraction between chlorine adatoms associated with the indirect interaction results in that the interatomic distance of 4.4 Å turns out beneficial, which gives rise to the formation of chains at low coverages, why is this distance no more optimum as the coverage degree increases to 0.3? On the other hand, if the adatoms separated by a distance of 5.0 Å attract one another, why is the formation of larger islands with the $(\sqrt{3} \times \sqrt{3})R30^\circ$ structure not observed at low coverages? To answer these questions, we simulated the formation of the structures concerned, by applying the Monte-Carlo method. The simulation was carried out using the lattice-gas model, the application of which in this case was completely justified owing to the circumstance that chlorine adatoms occupy almost equivalent *fcc* and *hcp* adsorption centers

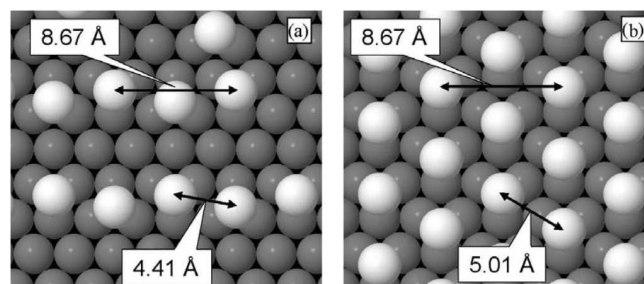


Fig. 1. Chains of chlorine adatoms (*a*) and the $(\sqrt{3} \times \sqrt{3})R30^\circ$ structure (*b*) on the Ag(111) surface

of threefold symmetry on the Ag(111) surface (the binding energy difference for chlorine in *fcc* and *hcp* centers is lower than 0.01 eV [10, 15]).

2. Calculation Technique

The lateral interaction energy was calculated in the framework of electron density functional theory, by taking advantage of the ABINIT software package [18] and using norm-conserving pseudopotentials [19] and the exchange-correlation potential in the generalized density gradient approximation [20]. Calculations for the surface concerned were carried out in the model of alternating layers with chlorine atoms adsorbed onto one layer side. A unit cell consisted of four atomic Ag(111) planes, a layer of adsorbed chlorines, and a vacuum gap 10 Å in thickness. The lateral interaction between Cl adatoms adsorbed on the Ag(111) surface was calculated using a 3×3 surface unit cell.

The positions of adsorbed chlorine atoms and two upper layers of the Ag(111) surface were optimized until the force acting upon the atoms became lower than 0.03 eV/Å. The efficiency of a Brillouin zone partition was checked using various lattices for \mathbf{k} -points needed to reach a convergence of 0.01 eV for the total energy and 0.01 Å for the atomic positions. For the 3×3 surface unit cell, the required convergence was attained, when using a set of $3 \times 3 \times 1$ special points [21]. All calculations were carried out using a cut-off energy of 30 Hartree. A more detailed description of the methods applied to compute the binding and lateral interaction energies can be found in works [15, 16, 22].

The Monte-Carlo simulation of the formation of chlorine structures on the Ag(111) surface was carried out taking advantage of original programs verified by simulating the formation of ordered structures in various adsorption systems [15, 16, 22–26]. This method implemented the standard Metropolis algorithm for the lattice gas model and took into account the long-range lateral interaction between particles adsorbed on the Ag(111) surface. The latter was presented as a 60×36 grid of adsorption centers, which corresponded to a surface area of about $100 \times 100 \text{ Å}^2$, with imposed periodic boundary conditions. The particles were ordered by shifting a randomly chosen adatom to the neighbor adsorption center making allowance for the existing diffusion barrier. The particle displacement probability at a given temperature T is determined by the expression $\exp(-\frac{\Delta E}{kT})$, where ΔE is the difference between the energies of lateral interaction with other adsorbed atoms in the initial and final configurations. The particle shift to the next center was

realized, if it was energetically beneficial for the system ($\Delta E < 0$) or if the displacement probability exceeded a generated random number. Otherwise, the system remained to stay in the initial configuration. As a result of a considerable number (10^5) of statistical tests, the thermodynamically equilibrium configuration of the adsorbed layer was attained.

If the temperature is lower than that of the order-disorder transition, the final layer structure corresponds to that, at which the energy of lateral interaction is minimal. At higher temperatures, fluctuations (energetically unprofitable displacements) play an important role, which brings about the layer disordering.

3. Results of Calculations

To carry out the simulation, it is necessary to determine the energies of lateral interaction at various interatomic distances. The distances between Cl adatoms located at *fcc* and *hcp* centers on the Ag(111) surface are, in the ascending order, 1.67, 2.89, 3.34, 4.41, 5.01, and 5.78 Å for first six neighbors. A straightforward calculation from the first principles is actually confined by the dimensions of a surface unit cell, at which such a calculation is feasible in practice, and by the restricted accuracy of calculations (of the order of a few millielectronvolts), whereas the formation of rarefied structures requires to consider the lateral interaction at much longer distances. Moreover, the first-principles calculations turned out very sensitive to relatively small variations in energy parameters.

The chain formation testifies that, besides the dipole-dipole repulsion $2\mu^2/r^3$, where r is the distance between adatoms and μ is the dipole moment, there exists the attraction between chlorine adatoms, probably owing to the indirect interaction through the electron subsystem of the surface, $V(r) \sim \cos(2k_F r + \delta)/r^n$ [27–29]. The period of Friedel oscillations [30] is determined by the Fermi vector k_F , and the phase shift δ fixes the position of the first minimum in the potential. The asymptotics of the indirect interaction depends on the dimensionality of a system and the Fermi surface shape. For instance, for free electrons in bulk, Lau and Kohn [28] predicted such an oscillating interaction, which depends on the distance as $1/r^5$, so that the interaction between adsorbed particles governed by bulk-electron states decreases much quicker than the dipole-dipole and elastic ones and, consequently, cannot be used to explain the formation of long-period structures. However, it should be noted that the damping asymptotics $1/r^5$ is valid only in the case of isotropic Fermi surfaces.

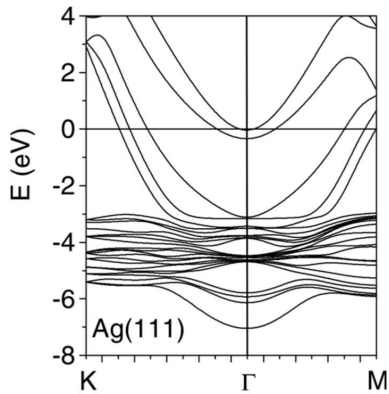


Fig. 2. Band structure of Ag(111). The Fermi wave vector averaged over the directions $k_F \approx 0.5 \text{ \AA}^{-1}$

As was shown by Lau and Kohn [28], the screening in a two-dimensional electron gas has a long-range character with the damping asymptotics $1/r^2$. Such a 2D gas of almost free electrons is realized in the surface states of densely packed surfaces in precious metals. Those states are localized near the center of the first Brillouin zone, so that very small wave vectors correspond to them. Therefore, the wavelength of Friedel oscillations associated with surface states is much longer than that for the bulk states [31–37]. In particular, the calculated band structure for the Ag(111) surface gives a surface state with $k_{F,\text{surf}} = 0.083 \text{ \AA}^{-1}$ [31]. This value corresponds to a period of Friedel oscillations of about 38 \AA , which is in agreement with the wavelength of surface charge density waves observed on this surface [33] and with the position of the first minimum for the lateral interaction potential on the Ag(111) surface (27 \AA for Co and 32 \AA for Ce [33, 34]).

It is evident that such a large period of potential oscillations, which is associated with the small Fermi vector for surface electron bands, does not allow it to be used for the explanation of the formation of structures in adsorbed layers with considerably shorter interatomic distances. On the other hand, the Fermi wave vector of electrons in the Ag bulk averaged over the directions equals 1.2 \AA^{-1} [37], which also looks hardly suitable to estimate the interaction on the surface. In addition, the interaction asymptotics $1/r^5$, which is inherent to Friedel oscillations in the case of spherical Fermi surface, testifies to its inefficiency at distances larger than a few lattice constants.

The solution of the problem was found in recent works by Silkin *et al.* [38]. The cited authors carefully calculated the charge density oscillations induced by an external excitation (adsorption) at the Cu(111) surface. The

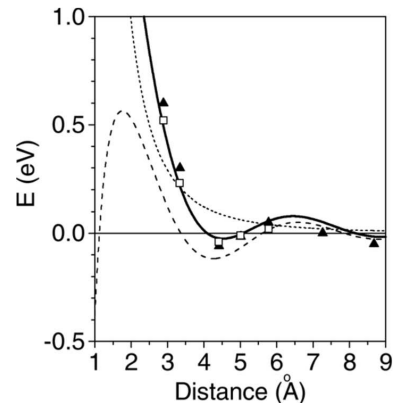


Fig. 3. Effective potential of the lateral interaction (solid curve), calculated interaction energies (squares), and parameters used in the Monte-Carlo simulation (triangles). Potential components: dipole – dipole (dotted curve) and indirect (dashed curve) interactions

calculations were carried out in the framework of linear response theory. The coexistence of 3D and 2D electron systems (the bulk electrons and the s - p_z surface bands that form a two-dimensional electron system, respectively) was made allowance for. The major result of the cited work was a convincing substantiation that such a coexistence of 3D and 2D electron systems considerably affects the induced oscillations of the electron density in the near-surface region, which brings about the $1/r^2$ -asymptotics in both electron subsystems in the static-excitation limit. Hence, the surface- and bulk-electron subsystems are not independent, and neglecting the role of bulk electrons in the screening of charged atom on the surface is rather a crude approximation. Whence it also follows that the k_F -value corresponding to the region, where the projection of bulk-electron bands (or separate bands obtained while calculating in the model of alternating layers) intersects the Fermi level (Fig. 2), may be the most suitable for the estimation of the oscillation period. The estimation for the Ag(111) surface gives k_F ranging from 0.5 to 0.8 \AA^{-1} , which corresponds to the potential oscillation period varying from 6.28 to 3.93 \AA , respectively. Just this order of magnitude is inherent to the interatomic distances in chlorine structures formed on the Ag(111) surface [9]. This fact testifies in favor of the explanation regarding their formation as a result of the indirect interaction with the participation of bulk electrons, which has the same asymptotics as the interaction associated with Friedel oscillations in a two-dimensional electron gas, i.e., $1/r^2$. Note also that the validity of the choice made for the effective potential form and the asymptotics $1/r^2$ for the indirect interaction was confirmed both experimentally [33] and by us-

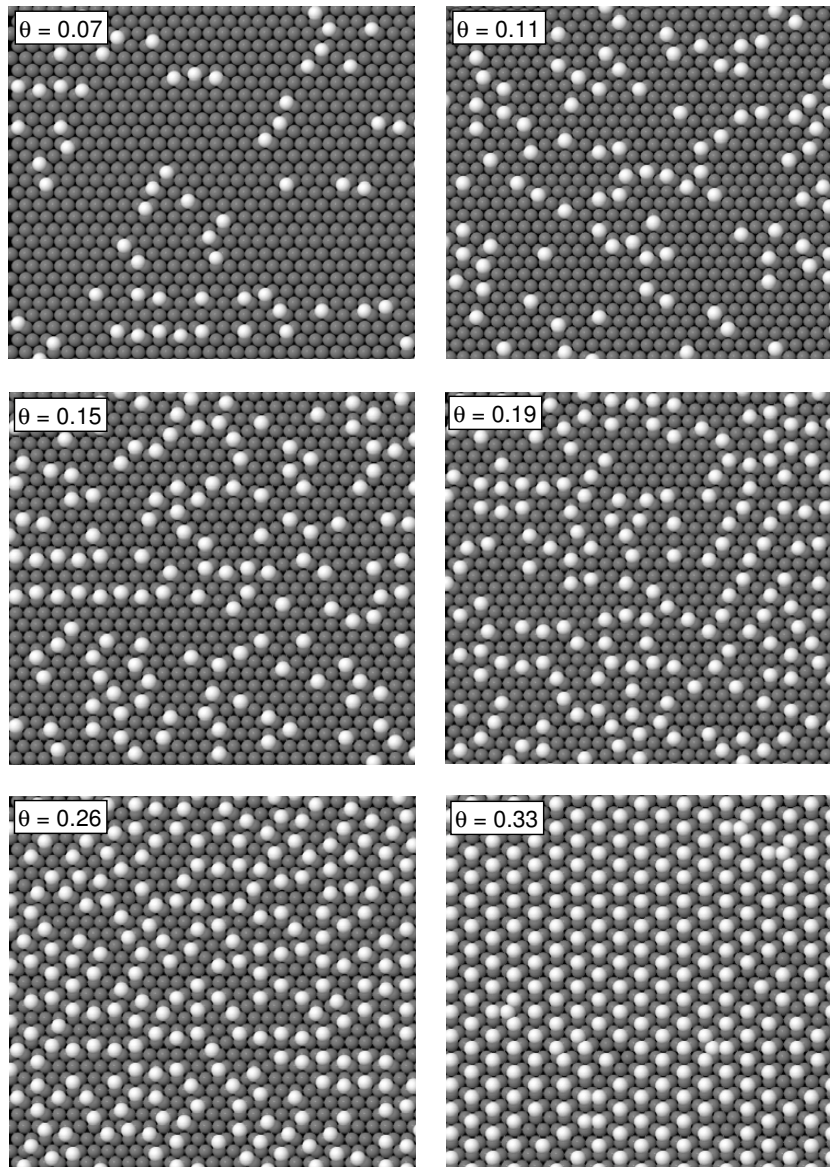


Fig. 4. Structure patterns obtained by the Monte-Carlo simulation. Chains of Cl adatoms are formed at low coverages. As the coverage increases, the $(\sqrt{3} \times \sqrt{3})R30^\circ$ structure is formed

ing the Monte-Carlo simulation of the formation of CO structures on the Pt(111) surface [24].

We adopted the effective potential of the lateral interaction, $V(r)$, between chlorine adatoms on the Ag(111) surface as a sum of the dipole-dipole and indirect interaction energies,

$$V(r) = \frac{2\mu^2}{1.6r^3} + \frac{A}{r^2} \cos(2k_F r + \delta). \quad (1)$$

The amplitude A and the dipole moment μ (a coefficient of 1.6 in the denominator of the first term allowed the

value of potential energy to be obtained in electronvolt units, if μ was expressed in Debye units) were specifically chosen to provide the best correspondence between the resulting effective potential and the lateral interaction energies calculated from the first principles (Fig. 3).

We simulated the structure patterns formed by chlorine adatoms at various coverage degrees, provided that the temperature is low enough. The results are presented in Fig. 4. In full correspondence with the experiment [9], if the coverage was low, the chain fragments were formed with an interatomic distance of

4.41 Å. When the degree of Ag(111) surface coverage approached 0.33, a commensurable $(\sqrt{3} \times \sqrt{3})R30^\circ$ lattice of chlorine atoms with interatomic distances of 5.01 Å emerged.

It is of interest to analyze the mechanism of transformation of chain structures into the $(\sqrt{3} \times \sqrt{3})R30^\circ$ one. An interatomic distance of 8.67 Å is characteristic of both those structures: being reckoned along the chain for the former and along six equivalent directions for the latter (Figs. 1, *a* and *b*). The lateral attraction is actual at this distance between adatoms (Fig. 3), which is responsible for the formation of the structures concerned. At low coverage degrees, the most beneficial distance between chlorine adatoms located on the Ag(111) surface at the adsorption centers of threefold symmetry is a distance of 4.41 Å (see Fig. 1). Therefore, the staggered chains are formed, in which atoms alternatively occupy *fcc* and *hcp* centers. As the coverage degree increases, the distance between the chains diminishes, so that a situation ultimately arises, when a displacement of every second atom in the chain into its neighbor adsorption center results in the formation of a $(\sqrt{3} \times \sqrt{3})R30^\circ$ structure with an interatomic distance of 5.01 Å. At this distance between adatoms, they also attract each other (Fig. 3), although the attraction is weaker than it was at the 4.41-Å separation. However, every atom in the $(\sqrt{3} \times \sqrt{3})R30^\circ$ structure has six neighbors located at identical (beneficial) distances of 5.01 Å, whereas an atom in the chain has only two corresponding neighbors. Therefore, a weakening of the attractive interaction between atoms in the $(\sqrt{3} \times \sqrt{3})R30^\circ$ structure becomes compensated by an increase in the number of atoms interacting at a distance of 5.01 Å, so that the $(\sqrt{3} \times \sqrt{3})R30^\circ$ structure turns out energetically more beneficial, as the coverage degree attains a value of 0.33.

4. Conclusions

The Monte-Carlo simulation with the use of the lateral interaction parameters calculated in the framework of electron density functional theory demonstrated that the chain formation is connected with the indirect interaction between chlorine adatoms. The results obtained allow us to explain the formation of a sequence of chlorine structures on the Ag(111) surface, which is observed in STM experiments. In particular, the interaction between adsorbed atoms was shown to be described well by a model that includes the dipole–dipole interaction and the interaction associated with Friedel oscillations of the electron density. The results obtained in the simulation enabled us to explain the transformation of a chain struc-

ture into a hexagonal one accompanied by an increase in the distance between the nearest chlorine atoms, which is experimentally observed, when the adatom concentration grows.

The work was executed in the framework of Ukrainian–Russian grant of the National Academy of Sciences of Ukraine and the Russian Fund for Basic Research No. RFBR/3-11-26.

1. G. Rovida and F. Pratesi, *Surf. Sci.* **51**, 270 (1975).
2. P.J. Goddard and R.M. Lambert, *Surf. Sci.* **67**, 180 (1977).
3. M. Bowker and K.C. Waugh, *Surf. Sci.* **134**, 639 (1983); K. Wu, D. Wang, J. Deng, X. Wei, Y. Cao, M. Zei, R. Zhai, and Z. Gao, *Surf. Sci.* **264**, 249 (1992).
4. B.V. Andryushechkin, K.N. Eltsov, V.M. Shevlyuga, and V.Yu. Yurov, *Surf. Sci.* **407**, L633 (1998); **431**, 96 (1999).
5. A.G. Shard and V.R. Dhanak, *J. Phys. Chem. B* **104**, 2743 (2000).
6. G.M. Lamble, R.S. Brooks, S. Ferrer, D.A. King, and D. Norman, *Phys. Rev. B* **34**, 2975 (1986).
7. J.H. Schott and H.S. White, *J. Phys. Chem.* **98**, 291 (1994).
8. B.V. Andryushechkin, V.V. Cherkez, E.V. Gladchenko, G.M. Zhidomirov, B. Kierren, Y. Fagot-Revurat, D. Malterre, and K.N. Eltsov, *Phys. Rev. B* **81**, 205434 (2010).
9. B.V. Andryushechkin, E.V. Gladchenko, K. Didieu, K.N. Eltsov, G.M. Zhidomirov, B. Kierren, and V.V. Cherkez, *Trudy IOF RAN* **66**, 20 (2010).
10. K. Doll and N.M. Harrison, *Phys. Rev. B* **63**, 165410 (2001).
11. Y. Wang, Q. Sun, K. Fan, and J. Deng, *Chem. Phys. Lett.* **334**, 411 (2001).
12. N.H. de Leeuw, C.J. Nelson, C.R.A. Catlow, P. Sautet, and W. Dong, *Phys. Rev. B* **69**, 045419 (2004).
13. A. Migani and F. Illas, *J. Phys. Chem. B* **110**, 11894 (2006).
14. P. Gava, A. Kokalj, S. Gironcoli, and S. Baroni, *Phys. Rev. B* **78**, 165419 (2008).
15. N.V. Petrova, I.N. Yakovkin, and O.M. Braun, *Chem. Phys.* **383**, 35 (2011).
16. N.V. Petrova, I.N. Yakovkin, and O.M. Braun, *Ukr. Fiz. Zh.* **56**, 361 (2011).
17. H. Piao, K. Adib, and M.A. Barteau, *Surf. Sci.* **557**, 13 (2004).
18. X. Gonze, J.-M. Beuken, R. Caracas, F. Detraux, M. Fuchs, G.-M. Rignanese, L. Sindic, M. Verstraete, G. Zerah, F. Jollet, M. Torrent, A. Roy, M. Mikami, Ph. Ghosez, J.-Y. Raty, and D.C. Allan, *Comput. Mat. Sci.* **25**, 478 (2002).

19. N. Troullier and J. L. Martins, Phys. Rev. B **43**, 1993 (1991).
20. J.P. Perdew, K. Burke, and M. Ernzerhof, Phys. Rev. Lett. **77**, 3865 (1996).
21. H.J. Monkhorst and J.D. Pack, Phys. Rev. B **13**, 5188 (1976).
22. N.V. Petrova and I.N. Yakovkin, Phys. Rev. B **76**, 205401 (2007).
23. N.V. Petrova, I.N. Yakovkin, and Yu.G. Ptushinskii, Eur. Phys. J. B **38**, 525 (2004).
24. N.V. Petrova and I.N. Yakovkin, Surf. Sci. **578**, 162 (2005).
25. N.V. Petrova, I.N. Yakovkin, and Yu.G. Ptushinskii, Fiz. Nizk. Temp. **31**, 300 (2005).
26. S.M. Orlyk, S.O. Solovyov, N.V. Petrova, and I.N. Yakovkin, Ukr. J. Phys. Rev. **48**, 64 (2008).
27. T.L. Einstein, CRC Crit. Rev. Solid State Mater. Sci. **7**, 261 (1978); Surf. Sci. **75**, L161 (1978).
28. K.H. Lau and W. Kohn, Surf. Sci. **65**, 607 (1977); **75**, 69 (1978).
29. O.M. Braun and V.K. Medvedev, Sov. Phys. Usp. **32**, 328 (1989).
30. J. Friedel, Nuovo Cim. Suppl. **7**, 287 (1958).
31. O. Jeandupeux, L.Bürigi, A. Hirstein, H. Brune, and K. Kern, Phys. Rev. B **59**, 15926 (1999).
32. P. Hyldgaard and M. Persson, J. Phys.: Condens. Matter **12**, L13 (2000).
33. N. Knorr, H. Brune, M. Epple, A. Hirstein, M.A. Schneider, and K. Kern, Phys. Rev. B **65**, 115420 (2002).
34. N.N. Negulyaev, V.S. Stepanyuk, W. Hergert, H. Fangohr, and P. Bruno, Surf. Sci. **600**, L58 (2006).
35. M. Kulawik, H.-P. Rust, M. Heyde, N. Nilius, B.A. Mantooth, P.S. Weiss, and H.-J. Freund, Surf. Sci. **590**, L253 (2005).
36. J. Repp, F. Moresco, G. Meyer, K.-H. Rieder, P. Hyldgaard, and M. Persson, Phys. Rev. Lett. **85**, 2981 (2000).
37. Ch. Kittel, *Introduction to Solid State Physics* (Wiley, New York, 1995).
38. V.M. Silkin, I.A. Nechaev, E.V. Chulkov, and P.M. Echenique, Surf. Sci. **588**, L239 (2005).

Received 05.07.2011.

Translated from Ukrainian by O.I. Voitenko

АТОМНІ ЛАНЦЮЖКИ ХЛОРУ НА ПОВЕРХНІ Ag(111)

Н.В. Петрова, І.М. Яковкін, О.М. Браун

Резюме

Формування ланцюжкових структур хлору на поверхні Ag(111) досліджено методом Монте-Карло із використанням параметрів латеральної взаємодії, розрахованих методом теорії функціонала електронної густини. Показано, що формування ланцюжків зумовлене непрямою взаємодією між адатомами хлору, що є наслідком фріделівських осциляцій електронів провідності при екрануванні частково заряджених адатомів. Проведене моделювання дозволяє пояснити послідовність формування структур хлору на поверхні Ag(111), що спостерігаються в експерименті. Зокрема, з'ясовано механізм переходу від ланцюжкової до гексагональної структури $(\sqrt{3} \times \sqrt{3})R30^\circ$ при збільшенні ступеня покриття до $\theta = 0,33$.